

DESCRIPTION OF THE RITA PAYLOAD ABOARD ALAINSAT-1, A 3U EDUCATIONAL CUBESAT

A. Gongora^{1,2}, A. Perez-Portero^{1,2}, L. Fernandez^{1,2}, A. Garcia-Morilla¹, G. Gracia-Sola¹, L. Contreras-Benito¹, J. Ramos-Castro^{2,3}, A. Camps^{1,2,5}, and A.H. Jallad⁶

¹CommSensLab – UPC, Universitat Politècnica de Catalunya – BarcelonaTech, Spain

²Institute of Space Studies of Catalonia (IEEC) – CTE-UPC, Spain

³Dept. of Electronic Engineering – UPC, Universitat Politècnica de Catalunya – BarcelonaTech, Spain

⁴ASPIRE Visiting International Professor, UAE University, CoE, POBox 15551 Al-Ain, UAE

⁵National Space Science and Technology Center, UAE University, CoE, POBox 15551 Al-Ain, UAE

ABSTRACT

The Remote sensing and Interference detector with radiometry and vegetation Analysis (RITA) payload was selected in 2019 the 2nd GRSS Student Grand Challenge to fly onboard AlainSat-1, a 3U CubeSat developed at the National Space Science and Technology Center (NSSTC) in United Arab Emirates. RITA payload includes a passive Microwave Radiometer (MWR), a LoRa transceiver, and an hyper-spectral camera. The objective of the payload is to retrieve Earth Observation (EO) parameters such as: soil moisture, sea-ice thickness and concentration, among others. A Radio Frequency Interference (RFI) detection algorithm is also included to the payload to create interference maps in the received signals.

Index Terms— CubeSat, Earth Observation, LoRa, Multi-spectral imaging, Radiometry, Remote Sensing, RFI.

1. INTRODUCTION

Polar caps melting, sea level rising, desertification, or extreme weather phenomena are some of the consequences of climate change. RITA payload was proposed to the 2nd IEEE GRSS Student Grand Challenge by a team of students of the Polytechnic University of Catalonia (UPC) NanoSatLab. Its main objective is to provide updated maps from Earth for the study of some specific Essential Climate Variables (ECVs). RITA includes a MWR with RFI detection capabilities, an hyper-spectral camera, and a LoRa transceiver. The MWR subsystem relies on the experience gathered from previous space missions developed at the UPC NanoSatLab alongside other CubeSats such as FSSCat/³CAT-5 [1] and ³CAT-4 [2]. With respect to the LoRa transceiver and the hyper-spectral camera subsystems, they aim to improve the resolution and accuracy of the data acquired from the MWR by means of data down-scaling algorithms [3]. Moreover a RFI detection algorithm will detect and classify corrupted measurements [4].

2. PAYLOAD OVERVIEW

The RITA payload is based on a Commercial of-the-shelf (COTS) System-on-Module (SoM) which includes a Software Defined Radio (SDR) Radio-Frequency (RF) transceiver (ADRV9364), and a System on a Chip (SoC) with a dual-core ARM Cortex-A9 processor with the hardware programmability of an Field-Programmable Gate Array (FPGA) (Zynq-7020). One restriction that the payload had was the requirement to occupy the volume of a one unit of a CubeSat standard (i.e. 10 cm x 10 cm x 11.35 cm). However, the form factor that the ADRV9364-z7020 adopts is not compatible with the CubeSat standard rails used by the form factor of the PC/104 standard boards. To solve this problem a specific structure was designed and manufactured in order to serve as an interface adapter between the RITA payload and the



Fig. 1. View of the final RITA payload version that will fly onboard AlainSat-1 Subesat.

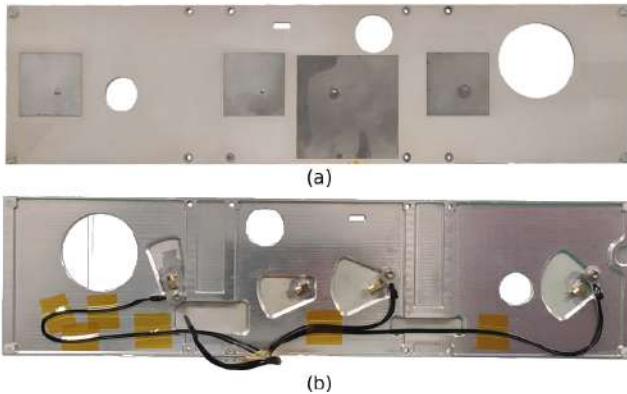


Fig. 2. RITA payload antenna (a) front view and (b) back view.

CubeSat platform (Fig. 1).

In the lower part of the payload there is a stack of PCBs all of them with the same form factor and interconnected. From top to bottom those are:

- The Front-End (FE) board.
- The Interface Board (IB).
- The COTS ADRV9364-z7020 board.

The IB in-house designed in which all the analogic and digital signal conditioning takes place together with power supply circuits. All the RF signal conditioning for the MWR and the LoRa transceiver takes place in the FE board also in-house designed. This board is enclosed by an aluminum shield for the minimization of RFI that could affect the performance of the experiments.

The hyper-spectral camera can be found in the upper part of the payload. Its camera lens is attached to the structure in the front, and also to an in-house manufactured internal baffle by means of a compatible C-mount. The baffle blocks and reduces any internal reflections towards the hyper-spectral image sensor. There are also two more PCBs stacked to the hyper-spectral sensor, one with an FPGA in charge of providing the discrete raw values from the hyper-spectral sensor, and another that interfaces with the sensor's FPGA and the RITA payload IB.

Furthermore, the RITA payload also includes an in-house manufactured antenna for the MWR and LoRa signal acquisition (Fig. 2). Made with RO4010 dielectric, it will cover one side of the 3U CubeSat (i.e. 32.54 cm x 8.26 cm). For the MWR, a Uniform Planar Array (UPA) formed by three micro-strip patch antennas will achieve a footprint resolution of 317 km in the cross-track direction and 1939 km in the along-track direction from a 560 km height Low Earth Orbit (LEO). For the LoRa transceiver, a single micro-strip patch antenna is enough to achieve the power link-budget [5].

3. SUBSYSTEMS DESCRIPTION

3.1. Microwave Radiometer

The MWR onboard the RITA payload is a Total Power Radiometer (TPR) operating at L-band ($f=1426$ MHz) [6]. TPRs can achieve good radiometric resolution despite being vulnerable to gain fluctuations of the receiving chain yielding to measurement errors. To mitigate these errors, a calibration subsystem with two internal loads, an Active Cold Load (ACL) and a matched load at ambient temperature, are used in such a way that a measurement from these two loads is done periodically for errors correction. The radiometric signal acquired by the UPA antenna is conditioned in a first instance by the FE board before reaching the SDR. The raw data is passed to the FPGA in charge of performing a level 0 signal processing storing the signal power. The physical antennas' temperature is measured and stored by means of NTC thermistors. Figure 3 shows the distribution of the MWR onboard RITA payload.

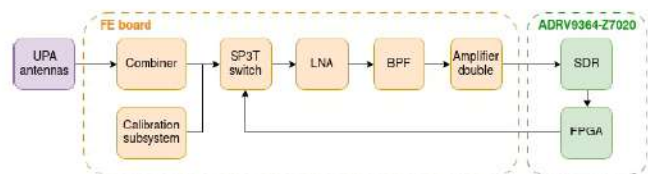


Fig. 3. TPR block diagram onboard RITA payload.

3.2. LoRa transceiver

The LoRa subsystem onboard RITA payload will be capable of transmitting and receiving information from a mesh of sensors distributed around the Earth in order to improve the EO maps obtained from the MWR and the hyper-spectral camera. Working at the region 1 Industrial, Scientific, and Medical (ISM) band (i.e. $f=868$ MHz), the signal will be either transmitted and received through the single patch antenna (Fig. 2). Thus, the RF signal will be conditioned in the FE board through the reception or the transmission chain selected by means of a commuting switch controlled by the FPGA. The SDR will record or transmit the raw data to/from the FPGA where the LoRa modulation/demodulation will take place (Fig. 4).

3.3. Hyper-spectral camera

The hyper-spectral sensor is a COTS from Photonfocus with 2048x1088 CMOS pixels, each of them with a dimension of 5.5 μm x 5.5 μm . An integrated 5x5 Fabry-Pérot filter array defines 25 pass bands ranging from 600 nm up to 975 nm wavelengths. During the image sensor characterization, it was realized that the response of the sensor in a specific band had an undesired secondary contribution outside the image sensor

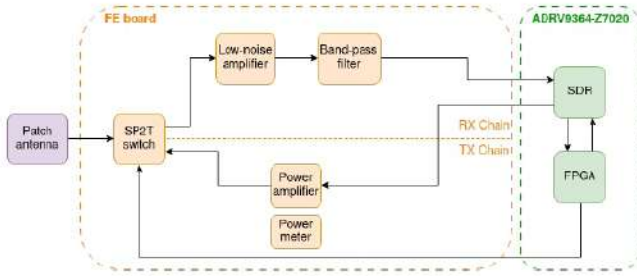


Fig. 4. LoRa block diagram onboard RITA payload.

bands coming from various channels. For its filtering, a Long Pass Filter (LPF) with a cut-off wavelength at 640 nm and a Short Pass Filter (SPF) with a cut-off wavelength at 850 nm have been added to the camera lens. The camera lens has been selected with a 16 mm focal length and an aperture of $f/1.4$ achieving an along-track resolution of 192.5 m for a 560 km height LEO.

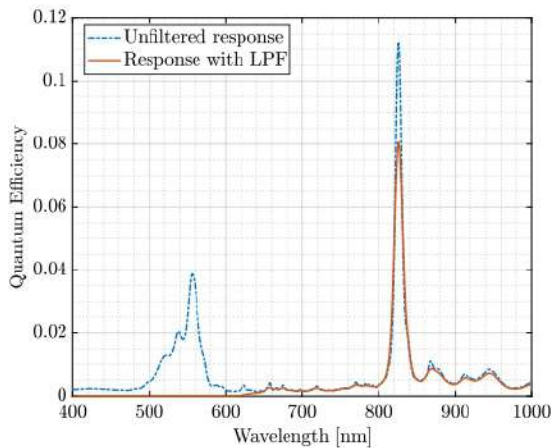


Fig. 5. Hyper-spectral 23rd band response without SPF (blue trace) and with SPF (orange trace).

The camera has an FPGA in charge of giving the discrete value of two consecutive pixels on each clock through twenty digital output pins. These values are routed towards the RITA's IB for its conditioning by means of level shifters, before going to the FPGA for its storing. Each pixel is quantized with 10 bits yielding approximately 2.8 MB of data per image.

4. ENVIRONMENTAL TESTING

In order to ensure that the payload will survive under the outer space conditions, an environmental test campaign was carried out inside a Thermal Vacuum Chamber (TVAC) at the UPC NanoSatLab facilities (Fig. 6). The TVAC is located inside an

ISO 7 clean room is not only capable to mimic vacuum conditions, but also to describe cold and hot temperature profiles defined by the operators.

The environmental test campaign for the Proto-Flight Model (PFM) payload was performed at acceptance level (i.e. from -10°C up to 55°C). All payload subsystems were verified during the environmental test campaign serving also for its characterization with temperature.

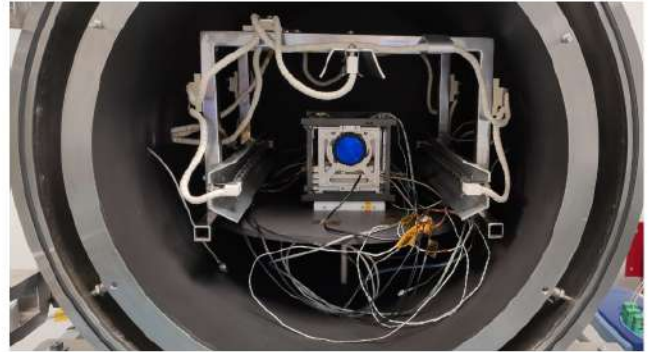


Fig. 6. RITA PFM payload inside the TVAC.

5. VIBRATIONS TESTING

Another important aspect is to ensure that the payload will withstand the launch conditions from the launch vehicle before reaching its orbit. A vibrations test campaign has been carried on RITA payload in a shake table at the UPC NanoSat-Lab facilities located inside an ISO 7 clean room. In a first instance, a qualification level campaign was performed over the Qualification Model (QM) payload before performing an acceptance level campaign over the PFM payload. Test profiles are defined by the launcher (i.e. Falcon9 from SpaceX) and the test sequence for each payload axis is the following one:

1. Resonance survey
2. Quasi-static load
3. Resonance survey
4. Random vibration
5. Resonance survey

During the first vibration test campaign it was realized that despite the first resonant frequency of the payload was around 900 Hz for each axis, which is far above the 100 Hz requirement where the mechanically transmitted energy from the launch vehicle is the dominant input for driving spacecraft responses, its amplitude was larger than $40\text{ g}^2/\text{Hz}$ for the random vibration test, compromising the payload's integrity.

To solve this issue, after several vibration analysis simulations made with Ansys, some modifications in the structure were performed in order to provide more stiffness to the payload. A new aluminum piece attaching the PCB stack from

Table 1. Summary of the vibration test results obtained for the initial structure design and the new structure design.

| | | QM PL old structure | | QM PL new structure | | PFM PL new structure | |
|--------|-----------------|---------------------|--------------------------------|---------------------|--------------------------------|----------------------|--------------------------------|
| | | f (Hz) | amplitude (g ² /Hz) | f (Hz) | amplitude (g ² /Hz) | f (Hz) | amplitude (g ² /Hz) |
| X-axis | First resonance | 820 | 1.84 | 947 | 0.95 | 925 | 0.84 |
| | Max resonance | 1322 | 29.80 | 1102 | 3.41 | 1080 | 4.65 |
| Y-axis | First resonance | 865 | 1.78 | 866 | 2.21 | 865 | 1.92 |
| | Max resonance | 993 | 41.32 | 987 | 23.30 | 993 | 18.60 |
| Z-axis | First resonance | 792 | 13.34 | 885 | 0.25 | 873 | 1.01 |
| | Max resonance | 1275 | 45.80 | 1442 | 3.92 | 1220 | 3.81 |

the FE board RF shield to the top side structure was added. Also the FE board RF shield was redesigned in order to be attached to the front and back sides of the structure, and the ribs in between the stack of PCBs were modified in such a way that two holes were added for its attachment to the bottom side. Finally, single piece and wider rods made of aluminum (7075-T6) were changed from previous ones composed by a 0.3 mm diameter threaded rod with aluminum (6061-T6) spacers.

From Table 1 it can be seen that the new structure gives more stiffness to the payload by slightly increasing the fundamental resonances for the X and Y axis with respect the initial structure version. Also the maximum resonance amplitudes were reduced notably in all the three axis.

6. CONCLUSIONS

At the time of writing this article, RITA payload has been fully characterized and verified not only under ambient conditions, but also during the environmental campaign and after the vibration campaign. A complete characterization of the Hyperspectral payload is presented in a companion paper [7]. It has been shipped to NSSTC in order to be assembled with the rest of the satellite.

7. ACKNOWLEDGEMENTS

This project is supported and funded by the IEEE Geoscience and Remote Sensing Society (GRSS), as one of the winners of the 2nd IEEE GRSS Student Grand Challenge, and supported grants for recruitment of early-stage research staff of Agència Gestió d'Ajuts Universitaris i de Recerca (AGAUR) Generalitat de Catalunya, Spain (FI2019/1183, FISDUR2020/105, FI2022/809, and FI2023/239). This article was part of the project "GENESIS: GNSS Environmental and Societal Missions – Subproject UPC", Grant PID2021-126436OB-C21 funded by the Ministerio de Ciencia e Investigación (MCIN)/Agencia Estatal de Investigación (AEI)/10.13039/501100011033 and EU FEDER "Una manera de hacer Europa".

8. REFERENCES

- [1] J. F. Munoz-Martin et al., "Soil Moisture Estimation Synergy Using GNSS-R and L-Band Microwave Radiometry Data from FSSCat/FMPL-2," *Remote Sensing*, vol. 13, no. 5, pp. 994, mar 2021.
- [2] J. F. Munoz-Martin et al., "3Cat-4: Combined GNSS-R, L-Band Radiometer with RFI Mitigation, and AIS Receiver for a I-Unit Cubesat Based on Software Defined Radio," in *IGARSS 2018 - 2018 IEEE International Geoscience and Remote Sensing Symposium*. jul 2018, IEEE.
- [3] Gerard Portal et al., "A Spatially Consistent Downscaling Approach for SMOS Using an Adaptive Moving Window," *IEEE Journal of Selected Topics in Applied Earth Observations and Remote Sensing*, vol. 11, no. 6, pp. 1883–1894, jun 2018.
- [4] J. Querol et al., "A Review of RFI Mitigation Techniques in Microwave Radiometry," *Remote Sensing*, vol. 11, no. 24, pp. 3042, dec 2019.
- [5] Lara Fernandez et al., "Assessing LoRa for Satellite-to-Earth Communications Considering the Impact of Ionospheric Scintillation," *IEEE Access*, vol. 8, pp. 165570–165582, 2020.
- [6] A. Gonga et al., "Design, Implementation, and Testing of a Microwave Radiometer for RITA, a 1U Payload on Board of the AlainSat-1," in *IGARSS 2022 - 2022 IEEE International Geoscience and Remote Sensing Symposium*, Kuala Lumpur, Malaysia, jul 2022.
- [7] L. Contreras-Benito et al., "Characterization and Verification of the RITA Payload Hyperspectral Imager in AlainSat-1, as part of the 2nd IEEE GRSS Student Grand Challenge," in *IGARSS 2023 - 2023 IEEE International Geoscience and Remote Sensing Symposium*, Pasadena, CA, USA, 2023 (in press), jul 2022.